Second Throat Diffuser Inlet Configuration for Steering Engine

A. Jeneev[1], M. Jegesh David[2], S. R. Balakrishnan[3]
PG scholar[1], Scientist HAT-C[2], Director
[1,3]Department of Aeronautical Engineering, Nehru institute of engineering and technology, [2]LPSC, Mahendragiri

Abstract

A second throat ejector using hydrogen and oxygen as the primary liquid is considered for the creation of a low vacuum in a high-altitude testing facility for large-area-ratio rocket steering engine .Detailed pressure investigations have been carried out to evaluate the performance of the second throat for various operational conditions and geometric parameters. When the diffuser attains started condition, supersonic flow fills the entire inlet section and a series of oblique shock cells occurring in the diffuser duct seal the vacuum environment of the test chamber against back flow. The most sensitive parameter with stagnation pressure needed for diffuser starting is the convergence angle. Between the throat and exit diameters of the nozzle, there exists a second-throat diameter value that corresponds to the lowest stagnation pressure for starting. When large radial/axial gaps exist between the nozzle exit and diffuser duct, significant reverse flow occurs for the unstarted cases, which spoils the vacuum in the test chamber. However, the starting stagnation pressure value remains unaffected by the axial/radial gap the suction pressure is influenced by the convergence angle. The predicted axial variations of static pressure along the diffuser are analyzed using ANSYS FLUENT and the modeled was carried out using CATIA V5.

Keywords - *High Altitude Test (HAT) facility, Second Throat Ejector- Diffuser (STED, Large area ratio satellite thruster, Back pressure.*

NOMENCLATURE

A_e = Thruster nozzle exit area
A_t = Thruster nozzle throat area
e = Specific internal energy
k = Thermal conductivity
M_i = Inlet Mach number
P_0 = Stagnation pressure
p = Static pressure
p_b = back pressure
pv = Vacuum chamber pressure
q = Heat transfer per unit area
r = radial coordinate
T_0 = Stagnation temperature
v = Velocity
z = Axial coordinate

1. Introduction

Propulsion systems are used to place spacecraft and artificial satellites in the desired orbits. Chemical thrusters are often employed as satellite propulsion systems for on- orbit control and station keeping. Satellites launched into orbit gradually tend to drift from the orbit both horizontally and vertically, due to atmospheric disturbances. For the Attitude and Orbital Control of Satellites (AOCS), small thrusters are mounted on the satellite which are designed to operate in upper atmosphere (high altitudes), where the pressure value is very low. The thrust levels for the thrusters employed in the satellite propulsion systems are very small in magnitude (in the range of few Newtons). During ground testing of such thrusters, the exhaust flow separates in the divergent portion of the nozzle due to large area ratio and resisting atmospheric pressure. Therefore, to attain full flow in the nozzle without any flow separation, the low pressure environment corresponding to the flight situation has to be created in the ground test facility. In the present study, an ejector-diffuser system is employed to create and maintain the required low pressure environment (about 3 mbar). Since the desired vacuum level is very low, a multi-stage external ejector is required to share the evacuation load. Also, the exhaust gas issued from the thruster does not have sufficient momentum to maintain the low pressure environment in the vacuum test chamber. Therefore, the maintenance of low vacuum level is achieved with the help of multi- stage ejector and the mild support of diffuser

2. High Altitude Test Facility

In general, a High Altitude Test (HAT) facility consists of various sub- systems like the large area ratio thruster which has to be tested, a vacuum chamber followed by a second throat diffuser and an external ejector system . Vacuum chamber is a vacuum holding device, which isolates the satellite thruster from outside ambient, by maintaining the low pressure value corresponding to the flight situation. The propellants stored at high stagnation pressure (P_0) and temperature (T_0) is allowed to expand through the large area ratio nozzle to produce high momentum rocket exhaust. The high velocity jet issued from the thruster impinges on the diffuser walls causing a series of oblique shocks, which terminates with a weak normal shock. These shock cells help in protecting the low vacuum level and also to achieve gradually pressure recovery. An external ejector is employed to create the low pressure environment corresponding to the high altitude flight situation.

The required vacuum level to operate the thruster without flow separation and the thrust generated by the thruster at full flow condition is about 37.447 mbar and . Since, the momentum of the exhaust gas is very low, the diffuser action (pressure recovery from low vacuum to a relatively higher pressure value) will not be appreciable. For achieving the above task (diffuser action and gas ejection), a single stage ejector may not be adequate; therefore, a two- stage ejector is required as shown in Fig. 1. Before igniting the thruster, the two- stage ejector system is alone operated to create the desired low vacuum. In the present study, simulations have been carried out assuming that the low vacuum level (~ 37.447 mbar) exists in the entire facility (vacuum chamber, thruster and diffuser portions). Geometry considered for the analysis is shown in (>>>>>>>>>>). The performance of the diffuser depends on both the upstream (rocket exhaust) and downstream (back pressure) conditions. The exhaust conditions corresponding to Ae/At = 56.5 is listed in Table 1. The ejector suction pressure (or diffuser back pressure) obtained from the ejector simulation

3. Modeling of Second Throat Ejector

Before the starting of the rocket motor, the vacuum chamber, diffuser, and the spray cooler portions will be evacuated to a very low pressure (37.447 mbar) with the help of the ejector. In this case, a low vacuum will prevail in the entire HAT facility, except across the ejector. The liquid rocket motor will be started with a slow increase in the flow rates of the propellants, and the water spray will be started when the temperature increase becomes significant.

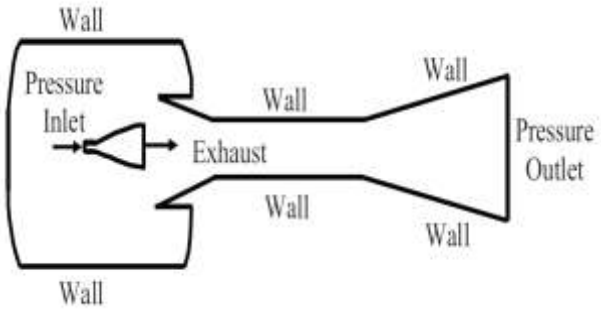

Figure 1 Geometry and boundary condition for analysis

4. Boundary conditions

The boundary conditions for the simulation (Fig. 1) are the prescribed in Table 1; no-slip and adiabatic conditions at the ejector wall; azimuthal symmetry on the axis; and a prescribed mass flux of primary Hydrogen flow (0.504 kg/s) at the ejector nozzle inlet with a stagnation temperature of 3200 K. This low-stagnation-temperature value for hydrogen flow takes into account the cooling experienced as hydrogen flows from the storage tanks through the piping. A segregated solver based on the SIMPLE technique is used to solve the aforementioned coupled partial differential equations, due to its faster convergence properties as compared with a fully coupled implicit compressible flow solver. Simulations have been carried out until the residues fall below 1 10 for all the flow variables. To investigate the sensitivity of the grid, a numerical investigation has been carried out for various mesh sizes ranging from 50,000 to computational domain and boundary conditions used for the 200,000 cells. The axial variation of static pressure predicted by different grids are almost identical (Fig. 3), indicating that the solution is insensitive to further grid refinement. Therefore, after detailed grid independence study a mesh with 150,000 cells has been adopted for all subsequent studies

Table 1 Boundary conditions

Condition	Value
Solver type	Pressure based
Model	K epsilon
Wall	No slip
Inlet Mach	5.2

Parameter	Values
Stagnation pressure, P bar	37
Stagnation temperature, T K	3200
Exit Mach number, M	5.2
Nozzle area ratio, A_e/A_t	56.5

5. Geometric parameters

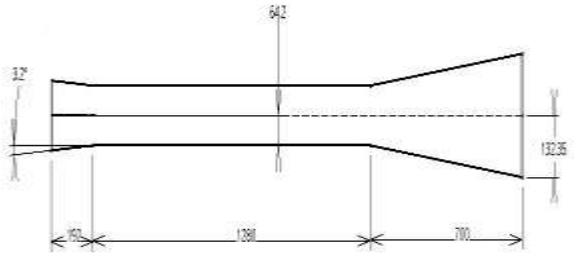

Figure 2: Second throat diffuser section

6. Numerical Methodology

The geometry and the boundary conditions used for the numerical simulations are shown in Fig. 2. The model is created using commercial software package GAMBIT and the governing equations are solved using finite volume technique based CFD solver (FLUENT 6.3). A segregated implicit solver with Spalart–Allmaras turbulence model has been adopted to compute the flow pattern inside the second throat ejector- diffuser system. The governing equations for the axi-symmetric compressible flow are presented below

Continuity equation:

$$\frac{1}{r}\frac{\partial}{\partial r}(\rho r v_r) + \frac{\partial}{\partial z}(\rho v_z) = 0$$

r- Momentum equation:

$$\rho\left(v_r\frac{\partial v_r}{\partial r} + v_z\frac{\partial v_r}{\partial z}\right) = -\frac{\partial p}{\partial r} - \left(\frac{1}{r}\frac{\partial}{\partial r}(r\tau_{rr}) + \frac{\partial \tau_{rz}}{\partial z}\right) + \frac{\tau_{\theta\theta}}{r}$$

z- Momentum equation:

$$\rho\left(v_r\frac{\partial v_z}{\partial r} + v_z\frac{\partial v_z}{\partial z}\right) = -\frac{\partial p}{\partial z} + \left(\frac{1}{r}\frac{\partial}{\partial r}(r\tau_{rz}) + \frac{\partial \tau_{zz}}{\partial z}\right)$$

Energy balance equation:

$$\rho\left(v_r\frac{\partial}{\partial r}(e+\frac{p}{\rho}) + v_z\frac{\partial}{\partial z}(e+\frac{p}{\rho})\right) = \frac{1}{r}\frac{\partial}{\partial r}(nq_r) - \frac{\partial q_z}{\partial z} + \mu\phi$$

$$\tau_{rr} = \mu\left[2\frac{\partial v_r}{\partial r} - \frac{2}{3}(\Delta.v)\right], \quad \tau_{rz} = \tau_{zr} = \mu\left[\frac{\partial v_z}{\partial r} + \frac{\partial v_r}{\partial z}\right]$$

$$\tau_{zz} = \mu\left[2\frac{\partial v_z}{\partial z} - \frac{2}{3}(\Delta.v)\right], \quad \tau_{\theta\theta} = \mu\left[2\frac{v_r}{r} - \frac{2}{3}(\Delta.v)\right]$$

$$q_r = -k\frac{\partial T}{\partial r}, \qquad q_z = -k\frac{\partial T}{\partial Z}$$

$$\phi = 2\left[\left(\frac{\partial v_r}{\partial r}\right)^2 + \left(\frac{\partial v_z}{\partial z}\right)^2\right] + \left[\frac{\partial v_r}{\partial z} + \frac{\partial v_z}{\partial r}\right]^2$$

7. Solution Methodology

A half-plane of the axisymmetric geometry is considered, from the axis to the wall of the second throat ejector system. The computational domain and boundary conditions used for the numerical analysis are shown in Fig. 2. The model is created using the commercial CFD package GAMBIT, and the governing equations are solved using FLUENT 6.2, which employs the finite Volume method to discretize the governing equations. A segregated implicit solver with the Spalart–Allamaras turbulence model has been adopted to compute the flow pattern inside the ejector system. In many compressible flow applications, as the temperature goes beyond 3000 K, the assumption of a calorifically perfect gas with constant properties becomes invalid. In the present case, the stagnation temperature is about 3200 K; therefore, the exhaust gas is assumed to behave as a thermally perfect gas. Hence, the fluid properties, such as specific heat, thermal conductivity, and viscosity, are considered to vary with temperature

8. Effect of Mixing Cone Convergent Angle

The variation of suction pressure during the different mixing cone convergent angle values in the range 2deg, 3 deg,7deg is presented in Fig. 12. It is to be noted that the length of the mixing cone (convergent portion) decreases with the increase in convergent angle. Figure 12 illustrates that, for a given hydrogen mass flux (.504 kg/s), the variation of suction pressure varies in the range of 2–30 mbar for 2 deg 8 deg. However, when the angle is increased up to 7 deg, the suction pressure increases 20 to 37.447 mbar. Such a rise in the suction pressure can be attributed to the shift in the location and the change in the angle of impact for the primary jet flow on the duct wall. So long as this angle of impact is small, the suction pressure is hardly affected. However, when increases, the jet impact becomes stronger, which results in stronger shock cells; hence, a deterioration occurs in the suction pressure value.

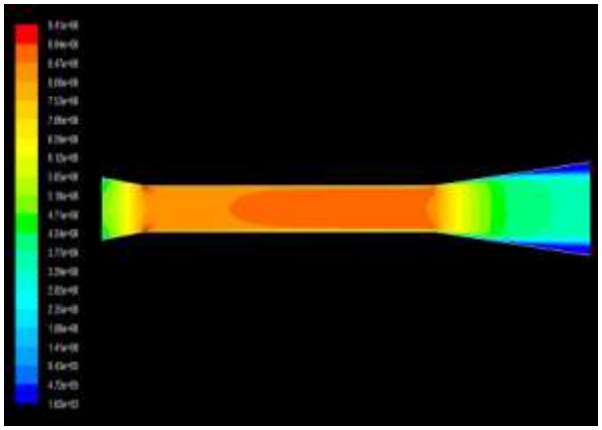

Figure3: Dynamic Pressure contour for Mach 5.2 with convergence angle 2 deg

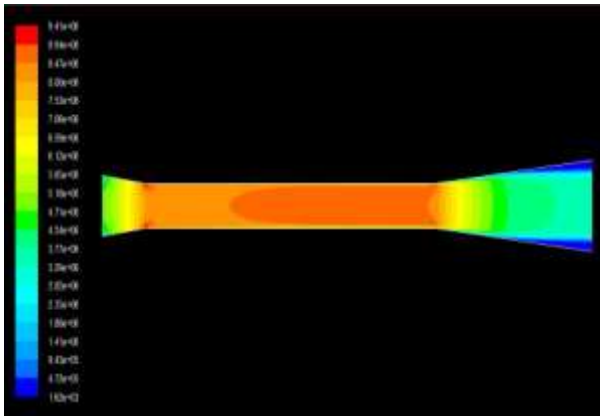

Figure6: Dynamic Pressure contour for Mach 5.2 with convergence angle 3 deg

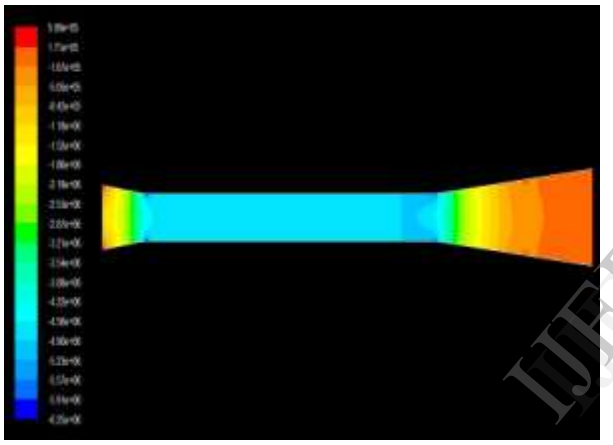

Figure 4: Static Pressure contour for Mach 5.2 with convergence angle 2 deg

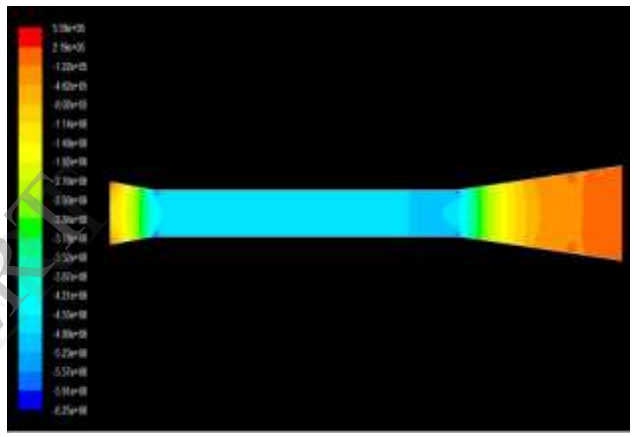

Figure7: Static Pressure contour for Mach 5.2 with convergence angle 3 deg

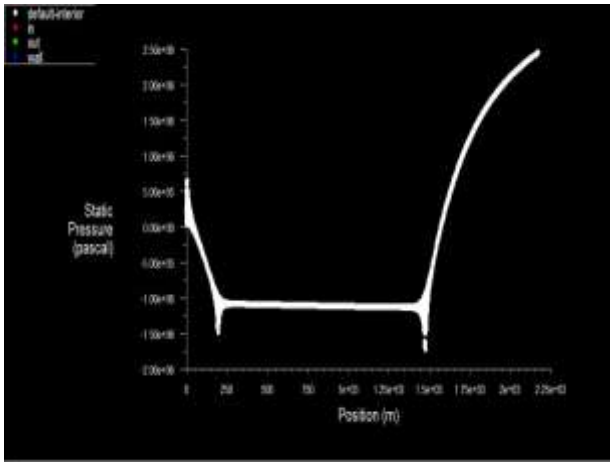

Figure: 5Graph for Pressure Vs Position at Angle 2 deg

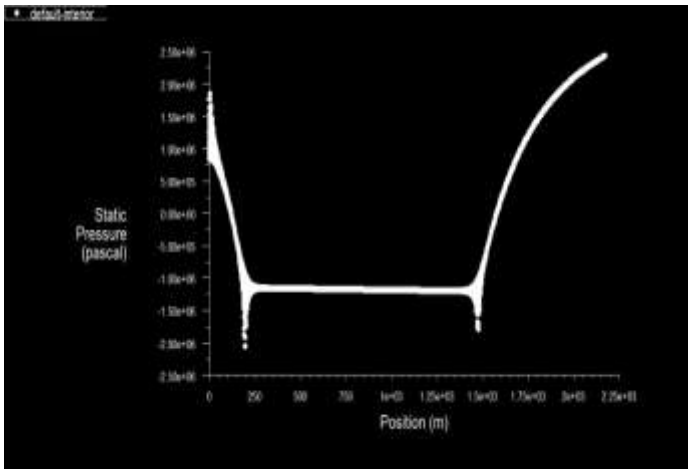

Figure 8: Graph for Pressure Vs Position at Angle 3 deg

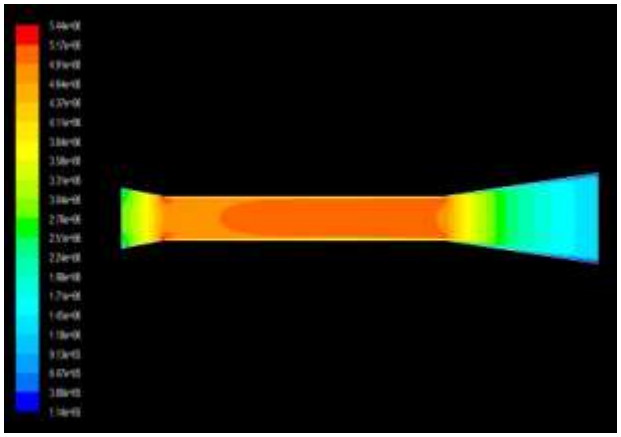

Figure9: Dynamic Pressure contour for Mach 5.2 with convergence angle 7 deg

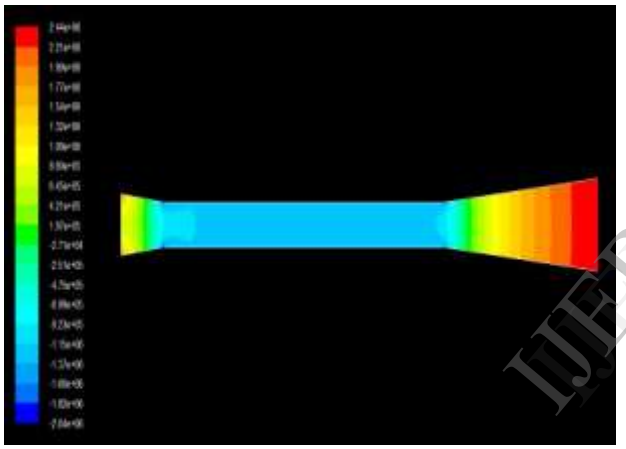

Figure10: Static Pressure contour for Mach 5.2 with convergence angle 7 deg

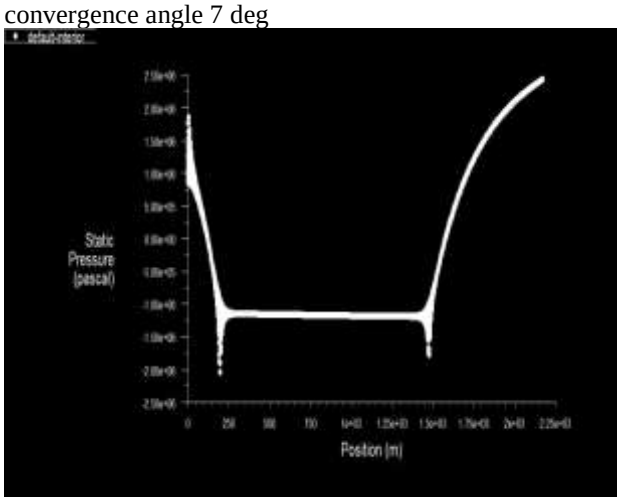

Figure11: Graph for Pressure Vs Position at Angle 7 deg

9. Variation of Angle influencing the pressure properties

The static-pressure contours shown in Fig. 5 for different Angle of inlet convergent portion shed more light on the phenomenon of diffuser starting. At low motor stagnation pressure the rocket plume does not have adequate momentum to drive the shock train out of the nozzle; consequently, the flow separates in the nozzle divergent portion. In such a situation, neither the nozzle nor the diffuser flows full. Because of reverse flow, the exhaust gas leaks into the test chamber through the small annular gap between the nozzle and diffuser wall and spoils the vacuum. As the stagnation pressure is increased, the exhaust flow fills the entire cross section of the nozzle, without any flow separation. The oblique shock attached to the lip of the nozzle gives rise to a series of reflected-shock cells that effectively seal the vacuum chamber from any backflow and help to maintain the low vacuum level (on the order of 37.447 mbar) in the test chamber. The oblique shock cells established in the diffuser duct also facilitate a gradual recovery of pressure.

10. Conclusion

This paper concludes that the effects of convergence angle variation (in the range of 2deg to 7deg) on the starting characteristics of the second-throat ejector–diffuser system are shown. Note that for fixed values of entry duct and second-throat diameters, the length of the convergent portion decreases with increasing angle. The performance of the second-throat ejector–diffuser system is hardly affected by the convergence angle. Both the starting stagnation-pressure value and the vacuum level achieved are essentially the same from 2deg to 7 deg. The diffuser for steering engine operating at a mach speed of 5.2 with inlet angle of 3 deg to 5 deg has the maximum suction pressure at the throat and thus the maximum recovery is obtained at the exit of the diffuser.

11. Reference

[1] Otters, T. M., Meyer, S., Heister, S., and Dambach, E., “Design of an Altitude-Testing Facility for Lab-Scale Propulsion Devices,” AIAA Paper 2007-5323, July 2007.

[2] Liu, Y. H., “Experimental and Numerical Research on High Pumping Performance Mechanism of Lobed Exhauster-Ejector Mixer,” International Communications in Heat and Mass Transfer, Vol. 34, No. 2, Feb. 2007, pp. 197–209.

[3] Nicholas, T. M. T., Narayanan, A. K., and Muthunayagam, A. E.,“Mixing Pressure-Rise Parameter for Effect of Nozzle Geometry inDiffuser-Ejectors,” Journal of Propulsion and Power, Vol. 12, No. 2,1996, pp. 431–433.

[4] Sankaran, S., Satyanarayana, T. N. V., Annamalai, K., Visvanathan, K.,Babu, V., and Sundararajan, T., "CFD Analysis for Simulated Altitude Testing of Rocket Motors," Canadian Aeronautics and Space Journal, Vol. 48, No. 2, June 2002, pp. 153–161.

[5] Puzach S.V., 1992. Effect of Supersonic Diffuser Geometry on Operation Conditions, Experimental Thermal and Fluid Science 5 124-128.

[6] Kim H., Lee Y., Setoguchi T. and Yu S., 1999. Numerical Simulation of the Supersonic Flows in the Second Throat Ejector- Diffuser Systems, Journal of Thermal Science 8 (4), 214-222.

[7] Annamalai, K., Viswanathan, K., Sriramulu, V., Bhaskaran, K.A., 1998. Evaluation of the performance of supersonic exhaust diffuser using scaled down models, Experimental Thermal and Fluid Science 78 217-229.

[8] Chen, F., Liu, C.F., Yang, J.Y., 1994. Supersonic flow in the second-throat ejectordiffuser system, Journal of Spacecraft and Rockets 31 (1) 123-129.

[9] Manikanda Kumaran R, Sundararajan T, David Dason, Raja Manohar D., October 2009. Ground Testing of Satellite Control Thrusters at High Altitude Conditions, International Conference on Applications and Design in Mechanical Engineering (ICADME 2009), Perlis, Malaysia.